8

A Complete Family of Kinematically-Simple Joint Layouts: Layout Models, Associated Displacement Problem Solutions and Applications

Scott Nokleby and Ron Podhorodeski

1. Introduction

Podhorodeski and Pittens (1992, 1994) and Podhorodeski (1992) defined a kinematically-simple (KS) layout as a manipulator layout that incorporates a spherical group of joints at the wrist with a main-arm comprised of successfully parallel or perpendicular joints with no unnecessary offsets or link lengths between joints. Having a spherical group of joints within the layouts ensures, as demonstrated by Pieper (1968), that a closed-form solution for the inverse displacement problem exists.

Using the notation of possible joint axes directions shown in Figure 1 and arguments of kinematic equivalency and mobility of the layouts, Podhorodeski and Pittens (1992, 1994) showed that there are only five unique, revolute-only, main-arm joint layouts representative of all layouts belonging to the KS family. These layouts have joint directions CBE, CAE, BCE, BEF, and AEF and are denoted KS 1 to 5 in Figure 2.

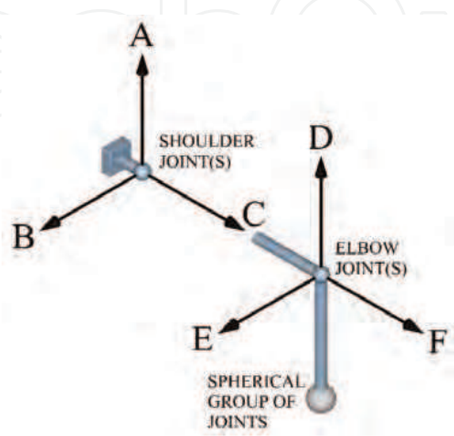

Figure 1. Possible Joint Directions for the KS Family of Layouts

Source: Industrial-Robotics-Theory-Modelling-Control, ISBN 3-86611-285-8, pp. 964, ARS/plV, Germany, December 2006, Edited by: Sam Cubero

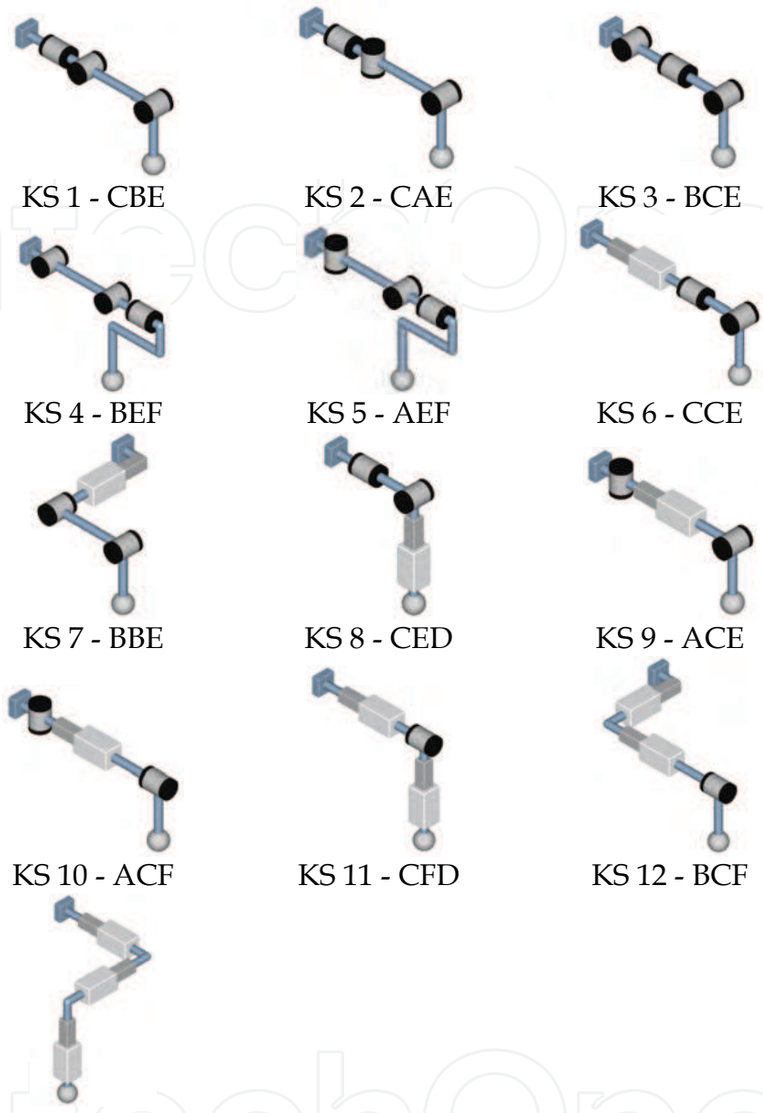

Figure 2. KS Family of Joint Layouts

Podhorodeski (1992) extended the work of Podhorodeski and Pittens (1992, 1994) to include prismatic joints in the layouts. Podhorodeski (1992) concluded that there are 17 layouts belonging to the KS family: five layouts comprised of three revolute joints; nine layouts comprised of two revolute joints and one prismatic joint; two layouts comprised of one revolute joint and two prismatic joints; and one layout comprised of three prismatic joints. However, four of the layouts comprised of two revolute joints and one prismatic joint (layouts he denotes AAE, AAF, ABF, and BAE) are not kinematically simple, by the definition set out in this chapter, due to an unnecessary offset existing between the second and third joints.

Yang et al. (2001) used the concepts developed by Podhorodeski and Pittens (1992, 1994) to attempt to generate all unique KS layouts comprised of two revolute joints and one prismatic joint. The authors identified eight layouts. Of these eight layouts, five layouts (the layouts they denote CAE, CAF, CBF, CFE, and CCE) are not kinematically simple, as defined in this chapter, in that they incorporate unnecessary offsets and one layout (the layout they denote CBE) is not capable of spatial motion.

The purpose of this chapter is to clarify which joint layouts comprised of a combination of revolute and/or prismatic joints belong to the KS family. The chapter first identifies all layouts belonging to the KS family. Zero-displacement diagrams and Denavit and Hartenberg (D&H) parameters (1955) used to model the layouts are presented. The complete forward and inverse displacement solutions for the KS family of layouts are shown. The application of the KS family of joint layouts and the application of the presented forward and inverse displacement solutions to both serial and parallel manipulators is discussed.

2. The Kinematically-Simple Family of Joint Layouts

The possible layouts can be divided into four groups: layouts with three revolute joints; layouts with two revolute joints and one prismatic joint; layouts with one revolute joint and two prismatic joints; and layouts with three prismatic joints.

2.1 Layouts with Three Revolute Joints

Using arguments of kinematic equivalency and motion capability, Podhorodeski and Pittens (1992, 1994) identified five unique KS layouts representative of all layouts comprised of three revolute joints. Referring to Figure 1, the joint directions for these layouts can be represented by the axes directions CBE, CAE, BCE, BEF, and AEF, and are illustrated as KS 1 to 5 in Figure 2, respectively.

Fundamentally degenerate layouts occur when either the three axes of the main arm intersect to form a spherical group (see Figure 3a) or when the axis of the final revolute joint intersects the spherical group at the wrist (see Figure 3b), i.e., the axis of the third joint is in the D direction of Figure 1. Note that for any KS layout, if the third joint is a revolute joint, the axis of the joint cannot intersect the spherical group at the wrist or the layout will be incapable of fully spatial motion.

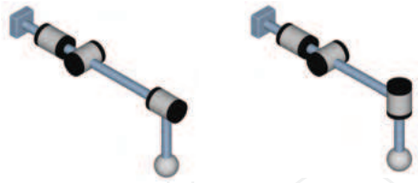

(a) Layout CBF (b) Layout CBD

Figure 3. Examples of the Two Types of Degenerate Revolute-Revolute-Revolute Layouts

2.2 Layouts with Two Revolute Joints and One Prismatic Joint

Layouts consisting of two revolute joints and one prismatic joint can take on three forms: prismatic-revolute-revolute; revolute-revolute-prismatic; and revolute-prismatic-revolute.

2.2.1 Prismatic-Revolute-Revolute Layouts

For a prismatic-revolute-revolute layout to belong to the KS family, either the two revolute joints will be perpendicular to one another or the two revolute joints will be parallel to one another. If the two revolute joints are perpendicular to one another, then the two axes must intersect to form a pointer, otherwise an unnecessary offset would exist between the two joints and the layout would not be kinematically simple. The prismatic-pointer layout can be represented by the axes directions CCE and is illustrated as KS 6 in Figure 2.
For the case where the two revolute joints are parallel to one another, in order to achieve full spatial motion, the axes of the revolute joints must also be parallel to the axis of the prismatic joint. If the axes of the revolute joints were perpendicular to the axis of the prismatic joint, the main-arm's ability to move the centre of the spherical group would be restricted to motion in a plane, i.e., fundamentally degenerate. In addition, a necessary link length must exist between the two revolute joints. The axes for this layout can be represented with the directions BBE and the layout is illustrated as KS 7 in Figure 2.

2.2.2 Revolute-Revolute-Prismatic Layouts

For a revolute-revolute-prismatic layout to belong to the KS family, either the two revolute joints will be perpendicular to one another or the two revolute joints will be parallel to one another. If the two revolute joints are perpendicular to one another, then the two axes must intersect to form a pointer, otherwise an unnecessary offset would exist between the two joints and the layout would not be kinematically simple. The pointer-prismatic layout can be represented by the axes directions CED and is illustrated as KS 8 in Figure 2.

For the case where the two revolute joints are parallel to one another, the axes of the revolute joints must also be parallel to the axis of the prismatic joint. In addition, a necessary link length must exist between the two revolute joints. The axes for this layout can be represented with the directions ADD. Note that for this configuration, the layout is fundamentally degenerate, unless an additional link length is added between joints two and three, since without the additional link length, the axis of the second revolute joint would always pass through the centre of the spherical joint group (see Figure 4a). Figure 4b illustrates the non-degenerate KS layout with an additional link length between the second revolute joint and the prismatic joint. However, the layout of Figure 4b is kinematically equivalent to KS 7 and therefore is not counted as a unique KS layout.

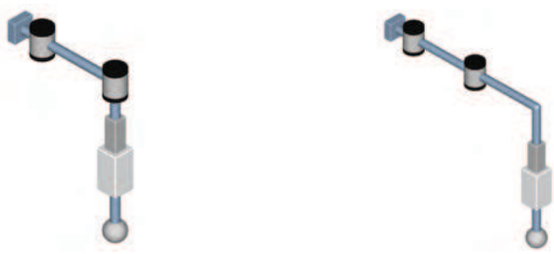

(a) Layout ADD (b) Layout ADD with Offset

Figure 4. Revolute-Revolute-Prismatic Layouts: a) Degenerate; b) Non-Degenerate

2.2.3 Revolute-Prismatic-Revolute Layouts

For a revolute-prismatic-revolute layout, in order to achieve spatial motion and belong to the KS class, the axes of the two revolute joints must be orthogonal to one another. The resulting KS layouts of axes can be represented by the axes directions ACE and ACF and are illustrated as KS 9 and KS 10 in Figure 2, respectively.

2.3 Layouts with One Revolute Joint and Two Prismatic Joints

Layouts consisting of one revolute joint and two prismatic joints can take on three forms: prismatic-revolute-prismatic; prismatic-prismatic-revolute; and revolute-prismatic-prismatic.

2.3.1 Prismatic-Revolute-Prismatic Layouts

For a prismatic-revolute-prismatic layout, the two prismatic joints must be perpendicular to each other. In order to achieve spatial motion and be kine-

matically simple, the axis of the revolute joint must be parallel to the axis of one of the prismatic joints. The feasible layout of joint directions can be represented by the axes directions CFD and is illustrated as KS 11 in Figure 2.

2.3.2 Prismatic-Prismatic-Revolute Layouts

For a prismatic-prismatic-revolute layout, the two prismatic joints must be perpendicular to each other. In order to achieve spatial motion and be kinematically simple, the axis of the revolute joint must be parallel to one of the prismatic joints. The feasible layout of joint directions can be represented by the axes directions BCF and is illustrated as KS 12 in Figure 2.

2.3.3 Revolute-Prismatic-Prismatic Layouts

For a revolute-prismatic-prismatic layout, the two prismatic joints must be perpendicular to each other. In order to achieve spatial motion and be kinematically simple, the axis of the revolute joint must be parallel to the axis of one of the prismatic joints. The feasible layout of joint directions can be represented by the axes directions CCD. Note that this layout is kinematically equivalent to the prismatic-revolute-prismatic KS 11. Therefore, the revolute-prismatic-prismatic layout is not kinematically unique. For a further discussion on collinear revolute-prismatic axes please see Section 2.5.

2.4 Layouts with Three Prismatic Joints

To achieve spatial motion with three prismatic joints and belong to the KS class, the joint directions must be mutually orthogonal. A representative layout of joint directions is CED. This layout is illustrated as KS 13 in Figure 2.

2.5 Additional Kinematically-Simple Layouts

The layouts above represent the 13 layouts with unique kinematics belonging to the KS family. However, additional layouts that have unique joint structures can provide motion that is kinematically equivalent to one of the KS layouts. For branches where the axes of a prismatic and revolute joint are collinear, there are two possible layouts to achieve the same motion. Four layouts, KS 6, 7, 11, and 12, have a prismatic joint followed by a collinear revolute joint. The order of these joints could be reversed, i.e., the revolute joint could come first followed by the prismatic joint. The order of the joints has no bearing on the kinematics of the layout, but would be very relevant in the physical design of a manipulator. Note that the d_j and θ_j elements of the corresponding rows in the D&H tables (see Section 3.2) would need to be interchanged along with

an appropriate change in subscripts. The presented forward and inverse displacement solutions in Sections 4.1 and 4.2 would remain unchanged except for a change in the relevant subscripts.

In addition to the above four layouts, as discussed in Section 2.2.2, the layout shown in Figure 4b is kinematically equivalent to KS 7. Therefore, there are five additional kinematically-simple layouts that can be considered part of the KS family.

3. Zero-Displacement Diagrams and D&H Parameters

3.1 Zero-Displacement Diagrams

The zero-displacement diagrams (θ_i = 0, for all revolute joints i) for the KS family of layouts for Craig's (1989) convention of frame assignment are presented in Figures 5 to 7. Note that the KS layouts in Figure 2 are not necessarily shown in zero-displacement. The rotations necessary to put each of the KS Layouts from zero-displacement configuration into the configuration illustrated in Figure 2 are outlined in Table 1.

KS	Rotations	KS	Rotations
1	$\theta_2 = \frac{\pi}{2}$	2	$\theta_2 = \frac{\pi}{2}$
3	$\theta_3 = \frac{\pi}{2}$	4	$\theta_2 = \frac{\pi}{2}$ & $\theta_3 = \frac{\pi}{2}$
5	$\theta_2 = -\frac{\pi}{2}$ & $\theta_3 = \frac{\pi}{2}$	6	$\theta_3 = -\frac{\pi}{2}$
7	None	8	$\theta_2 = -\frac{\pi}{2}$
9	$\theta_3 = \frac{\pi}{2}$	10	None
11	None	12	$\theta_3 = \frac{\pi}{2}$
13	None		

Table 1. Rotations Necessary to put Each of the KS Layouts from Zero-Displacement Configuration (Figures 5 to 7) into the Configuration Illustrated in Figure 2

3.2 D&H Parameters

Table 2 shows the D&H parameters for the kinematically-simple family of joint layouts. The D&H parameters follow Craig's frame assignment convention (Craig, 1989) and correspond to the link transformations:

$$
\begin{aligned}
{}^{j-1}_{j}\mathbf{T} &= Rot_{\hat{\mathbf{x}}_{j-1}}(\alpha_{j-1})\,Trans_{\hat{\mathbf{x}}_{j-1}}(a_{j-1})\,Trans_{\hat{\mathbf{z}}_j}(d_j)\,Rot_{\hat{\mathbf{z}}_j}(\theta_j) \\
&= \begin{bmatrix}
\cos(\theta_j) & -\sin(\theta_j) & 0 & a_{j-1} \\
\sin(\theta_j)\cos(\alpha_{j-1}) & \cos(\theta_j)\cos(\alpha_{j-1}) & -\sin(\alpha_{j-1}) & -\sin(\alpha_{j-1})d_j \\
\sin(\theta_j)\sin(\alpha_{j-1}) & \cos(\theta_j)\sin(\alpha_{j-1}) & \cos(\alpha_{j-1}) & \cos(\alpha_{j-1})d_j \\
0 & 0 & 0 & 1
\end{bmatrix}
\end{aligned}
\tag{1}
$$

where ${}^{j-1}_{j}\mathbf{T}$ is a homogeneous transformation describing the location and orientation of link-frame F_j with respect to link-frame F_{j-1}, $Rot_{\hat{\mathbf{x}}_{j-1}}(\alpha_{j-1})$ denotes a rotation about the $\hat{\mathbf{x}}_{j-1}$ axis by α_{j-1}, $Trans_{\hat{\mathbf{x}}_{j-1}}(a_{j-1})$ denotes a translation along the $\hat{\mathbf{x}}_{j-1}$ axis by a_{j-1}, $Trans_{\hat{\mathbf{z}}_j}(d_j)$ denotes a translation along the $\hat{\mathbf{z}}_j$ axis by d_j, and $Rot_{\hat{\mathbf{z}}_j}(\theta_j)$ denotes a rotation about the $\hat{\mathbf{z}}_j$ axis by θ_j.

The homogeneous transformation of equation (1) is of the form:

$$
{}^{j-1}_{j}\mathbf{T} = \begin{bmatrix}
{}^{j-1}_{j}\mathbf{R} & {}^{j-1}\mathbf{p}_{o_{j-1}\to o_j} \\
0 \quad 0 \quad 0 & 1
\end{bmatrix}
\tag{2}
$$

where ${}^{j-1}_{j}\mathbf{R}$ is a 3x3 orthogonal rotation matrix describing the orientation of frame F_j with respect to frame F_{j-1} and ${}^{j-1}\mathbf{p}_{o_{j-1}\to o_j}$ is a vector from the origin of frame F_{j-1} to the origin of frame F_j.

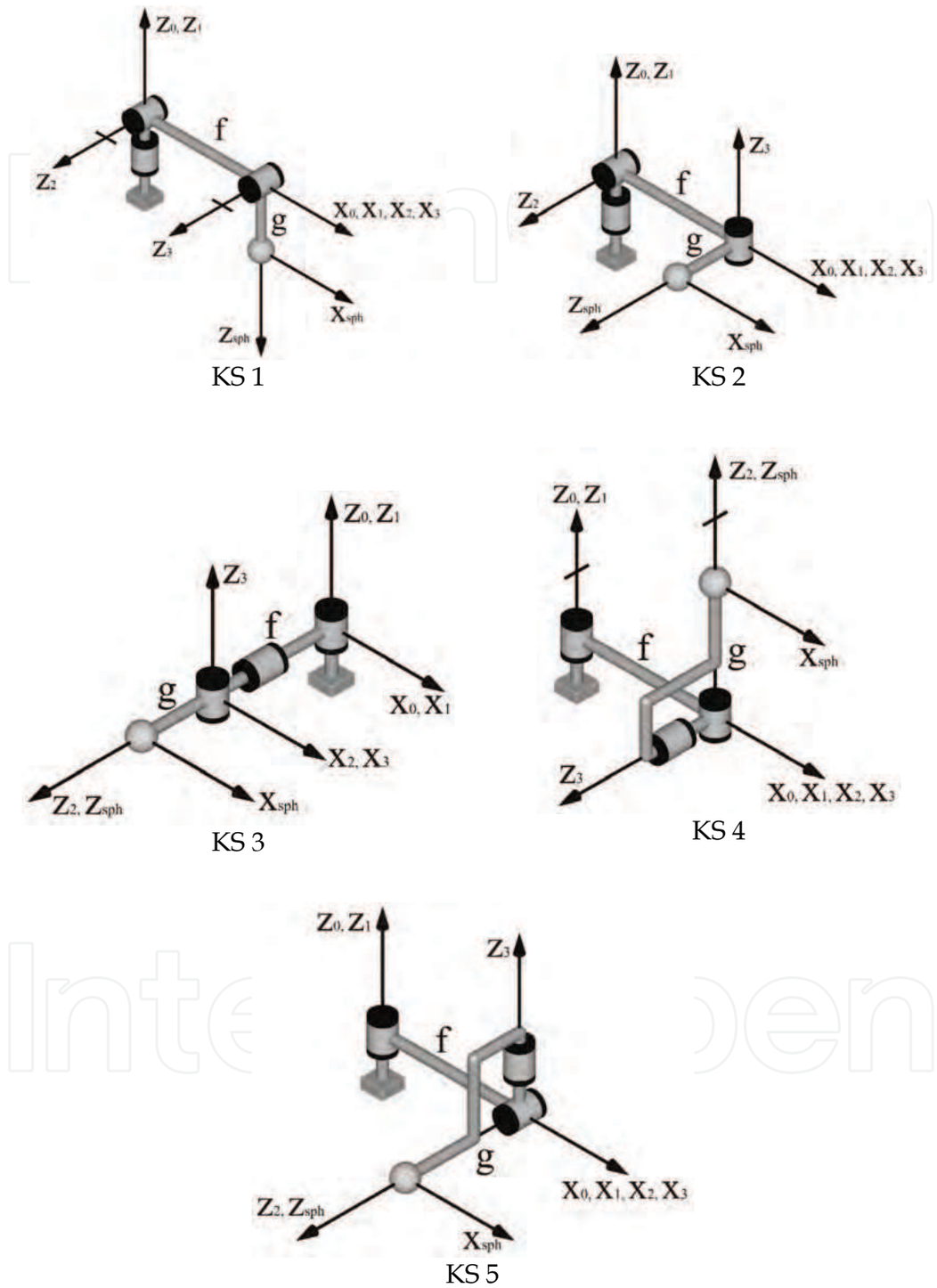

Figure 5. Zero-Displacement Diagrams for Layouts with Three Revolute Joints (KS 1 to 5)

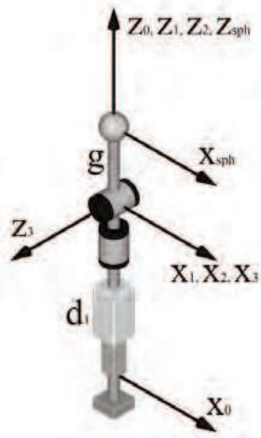

KS 6

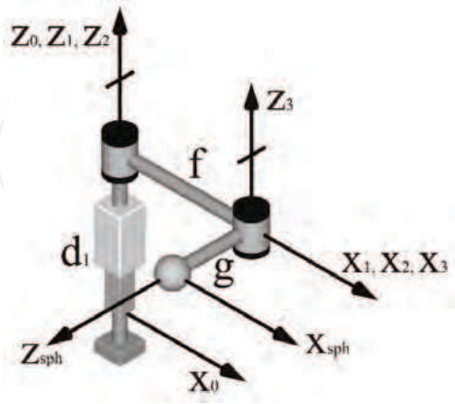

KS 7

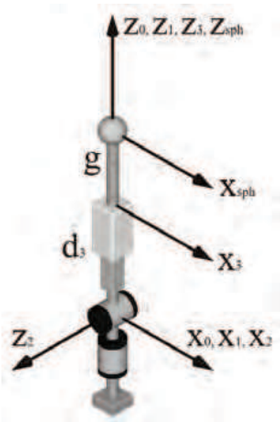

KS 8

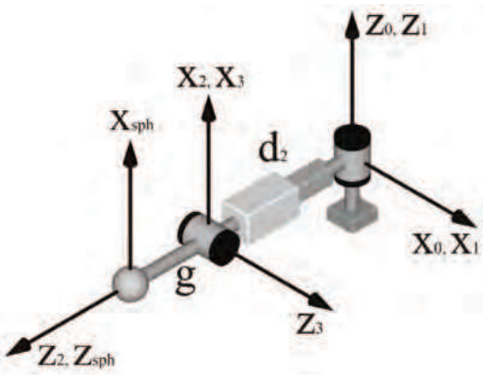

KS 9

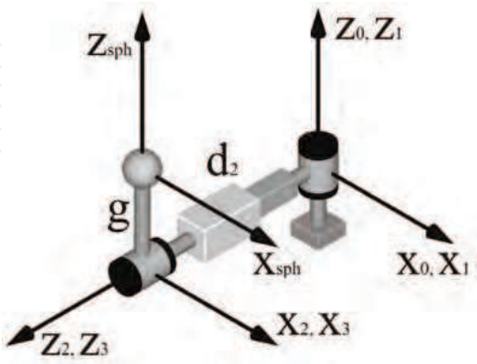

KS 10

Figure 6. Zero-Displacement Diagrams for Layouts with Two Revolute Joints and One Prismatic Joint (KS 6 to 10)

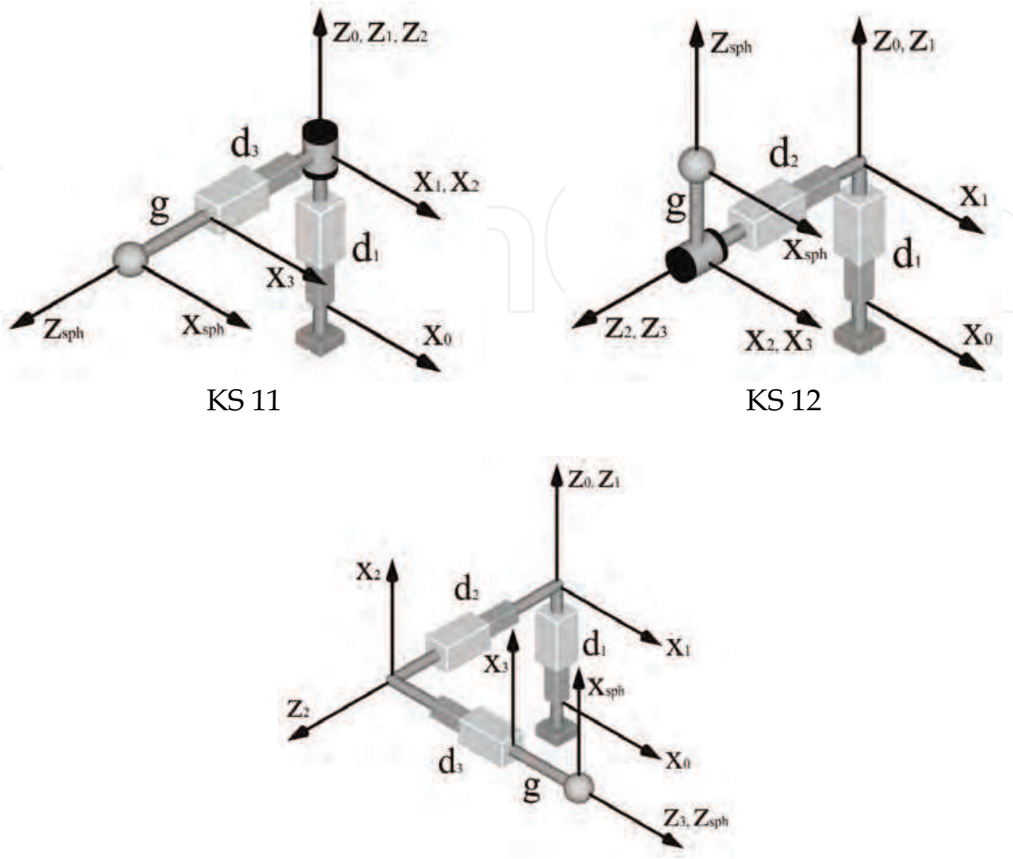

Figure 7. Zero-Displacement Diagrams for Layouts with One Revolute Joint and Two Primatic Joints (KS 11 and 12) or Three Prismatic Joints (KS 13)

4. Forward and Inverse Displacement Solutions

4.1 Forward Displacement Solutions for the KS Family of Layouts

The position and orientation of the spherical wrist frame F_{sph} with respect to the base frame F_0 is found from:

$$ {}^{0}_{sph}\mathbf{T} = {}^{0}_{1}\mathbf{T}\ {}^{1}_{2}\mathbf{T}\ {}^{2}_{3}\mathbf{T}\ {}^{3}_{sph}\mathbf{T} = \begin{bmatrix} {}^{0}_{sph}\mathbf{R} & {}^{0}\mathbf{p}_{o_0 \to o_{sph}} \\ 0 \quad 0 \quad 0 & 1 \end{bmatrix} \tag{3} $$

where the homogeneous transformation ${}^{j-1}_{j}\mathbf{T}$ is defined in equation (1). The transformation ${}^{0}_{sph}\mathbf{T}$ is the solution to the forward displacement problem: ${}^{0}_{sph}\mathbf{R}$

is the change in orientation due to the first three joints and ${}^{0}\mathbf{p}_{o_0 \to o_{sph}}$ is the location of the spherical wrist centre. The homogeneous transformations ${}^{0}_{sph}\mathbf{T}$ for the KS family of layouts can be found in Tables 3 and 4. Note that in Tables 3 and 4, c_i and s_i denote $\cos(\theta_i)$ and $\sin(\theta_i)$, respectively.

KS	F_{j-1}	α_{j-1}	a_{j-1}	d_j	θ_j	F_j	KS	F_{j-1}	α_{j-1}	a_{j-1}	d_j	θ_j	F_j
1	F_0	0	0	0	θ_1	F_1	2	F_0	0	0	0	θ_1	F_1
	F_1	$\pi/2$	0	0	θ_2	F_2		F_1	$\pi/2$	0	0	θ_2	F_2
	F_2	0	f	0	θ_3	F_3		F_2	$-\pi/2$	f	0	θ_3	F_3
	F_3	$\pi/2$	0	g	0	F_{sph}		F_3	$\pi/2$	0	g	0	F_{sph}
3	F_0	0	0	0	θ_1	F_1	4	F_0	0	0	0	θ_1	F_1
	F_1	$\pi/2$	0	f	θ_2	F_2		F_1	0	f	0	θ_2	F_2
	F_2	$-\pi/2$	0	0	θ_3	F_3		F_2	$\pi/2$	0	0	θ_3	F_3
	F_3	$\pi/2$	0	g	0	F_{sph}		F_3	$-\pi/2$	0	g	0	F_{sph}
5	F_0	0	0	0	θ_1	F_1	6	F_0	0	0	d_1	0	F_1
	F_1	$\pi/2$	f	0	θ_2	F_2		F_1	0	0	0	θ_2	F_2
	F_2	$-\pi/2$	0	0	θ_3	F_3		F_2	$\pi/2$	0	0	θ_3	F_3
	F_3	$\pi/2$	0	g	0	F_{sph}		F_3	$-\pi/2$	0	g	0	F_{sph}
7	F_0	0	0	d_1	0	F_1	8	F_0	0	0	0	θ_1	F_1
	F_1	0	0	0	θ_2	F_2		F_1	$\pi/2$	0	0	θ_2	F_2
	F_2	0	f	0	θ_3	F_3		F_2	$-\pi/2$	0	d_3	0	F_3
	F_3	$\pi/2$	0	g	0	F_{sph}		F_3	0	0	g	0	F_{sph}
9	F_0	0	0	0	θ_1	F_1	10	F_0	0	0	0	θ_1	F_1
	F_1	$\pi/2$	0	d_2	$\pi/2$	F_2		F_1	$\pi/2$	0	d_2	0	F_2
	F_2	$\pi/2$	0	0	θ_3	F_3		F_2	0	0	0	θ_3	F_3
	F_3	$-\pi/2$	0	g	0	F_{sph}		F_3	$-\pi/2$	0	g	0	F_{sph}
11	F_0	0	0	d_1	0	F_1	12	F_0	0	0	d_1	0	F_1
	F_1	0	0	0	θ_2	F_2		F_1	$\pi/2$	0	d_2	0	F_2
	F_2	$\pi/2$	0	d_3	0	F_3		F_2	0	0	0	θ_3	F_3
	F_3	0	0	g	0	F_{sph}		F_3	$-\pi/2$	0	g	0	F_{sph}
13	F_0	0	0	d_1	0	F_1							
	F_1	$\pi/2$	0	d_2	$\pi/2$	F_2							
	F_2	$\pi/2$	0	d_3	0	F_3							
	F_3	0	0	g	0	F_{sph}							

Table 2. D&H Parameters for the KS Layouts

KS	${}^{0}_{sph}\mathbf{T}$
1	$\begin{bmatrix} c_1c_{23} & s_1 & c_1s_{23} & c_1(c_2f+s_{23}g) \\ s_1c_{23} & -c_1 & s_1s_{23} & s_1(c_2f+s_{23}g) \\ s_{23} & 0 & -c_{23} & s_2f-c_{23}g \\ 0 & 0 & 0 & 1 \end{bmatrix}$
2	$\begin{bmatrix} c_1c_2c_3-s_1s_3 & -c_1s_2 & c_1c_2s_3+s_1c_3 & c_1c_2f+(c_1c_2s_3+s_1c_3)g \\ s_1c_2c_3+c_1s_3 & -s_1s_2 & s_1c_2s_3-c_1c_3 & s_1c_2f+(s_1c_2s_3-c_1c_3)g \\ s_2c_3 & c_2 & s_2s_3 & s_2f+s_2s_3g \\ 0 & 0 & 0 & 1 \end{bmatrix}$
3	$\begin{bmatrix} c_1c_2c_3-s_1s_3 & -c_1s_2 & c_1c_2s_3+s_1c_3 & s_1f+(c_1c_2s_3+s_1c_3)g \\ s_1c_2c_3+c_1s_3 & -s_1s_2 & s_1c_2s_3-c_1c_3 & -c_1f+(s_1c_2s_3-c_1c_3)g \\ s_2c_3 & c_2 & s_2s_3 & s_2s_3g \\ 0 & 0 & 0 & 1 \end{bmatrix}$
4	$\begin{bmatrix} c_{12}c_3 & -s_{12} & -c_{12}s_3 & c_1f-c_{12}s_3g \\ s_{12}c_3 & c_{12} & -s_{12}s_3 & s_1f-s_{12}s_3g \\ s_3 & 0 & c_3 & c_3g \\ 0 & 0 & 0 & 1 \end{bmatrix}$
5	$\begin{bmatrix} c_1c_2c_3-s_1s_3 & -c_1s_2 & c_1c_2s_3+s_1c_3 & c_1f+(c_1c_2s_3+s_1c_3)g \\ s_1c_2c_3+c_1s_3 & -s_1s_2 & s_1c_2s_3-c_1c_3 & s_1f+(s_1c_2s_3-c_1c_3)g \\ s_2c_3 & c_2 & s_2s_3 & s_2s_3g \\ 0 & 0 & 0 & 1 \end{bmatrix}$

Table 3. Forward Displacement Solutions for KS 1 to 5

4.2 Inverse Displacement Solutions for the KS Family of Layouts

For the inverse displacement solution, the location of the spherical wrist centre with respect to the base, ${}^{0}\mathbf{p}_{o_0\to o_{sph}}$, is known:

$$ {}^{0}\mathbf{p}_{o_0\to o_{sph}} = \begin{Bmatrix} p_x \\ p_y \\ p_z \end{Bmatrix} \tag{4} $$

Paul (1981) presented a methodology to solve the inverse displacement problem of 6-joint manipulators with a spherical wrist. To demonstrate the application of this methodology to the inverse displacement problem for the KS family, KS 1 will be used as an example.

KS	${}^{0}_{sph}\mathbf{T}$	KS	${}^{0}_{sph}\mathbf{T}$
6	$\begin{bmatrix} c_2c_3 & -s_2 & -c_2s_3 & -c_2s_3g \\ s_2c_3 & c_2 & -s_2s_3 & -s_2s_3g \\ s_3 & 0 & c_3 & c_3g+d_1 \\ 0 & 0 & 0 & 1 \end{bmatrix}$	7	$\begin{bmatrix} c_{23} & 0 & s_{23} & c_2f+s_{23}g \\ s_{23} & 0 & -c_{23} & s_2f-c_{23}g \\ 0 & 1 & 0 & d_1 \\ 0 & 0 & 0 & 1 \end{bmatrix}$
8	$\begin{bmatrix} c_1c_2 & -s_1 & -c_1s_2 & -c_1s_2(d_3+g) \\ s_1c_2 & c_1 & -s_1s_2 & -s_1s_2(d_3+g) \\ s_2 & 0 & c_2 & c_2(d_3+g) \\ 0 & 0 & 0 & 1 \end{bmatrix}$	9	$\begin{bmatrix} s_1s_3 & -c_1 & s_1c_3 & s_1(c_3g+d_2) \\ -c_1s_3 & -s_1 & -c_1c_3 & -c_1(c_3g+d_2) \\ c_3 & 0 & -s_3 & -s_3g \\ 0 & 0 & 0 & 1 \end{bmatrix}$
10	$\begin{bmatrix} c_1c_3 & -s_1 & -c_1s_3 & -c_1s_3g+s_1d_2 \\ s_1c_3 & c_1 & -s_1s_3 & -s_1s_3g-c_1d_2 \\ s_3 & 0 & c_3 & c_3g \\ 0 & 0 & 0 & 1 \end{bmatrix}$	11	$\begin{bmatrix} c_2 & 0 & s_2 & s_2(g+d_3) \\ s_2 & 0 & -c_2 & -c_2(g+d_3) \\ 0 & 1 & 0 & d_1 \\ 0 & 0 & 0 & 1 \end{bmatrix}$
12	$\begin{bmatrix} c_3 & 0 & -s_3 & -s_3g \\ 0 & 1 & 0 & -d_2 \\ s_3 & 0 & c_3 & c_3g+d_1 \\ 0 & 0 & 0 & 1 \end{bmatrix}$	13	$\begin{bmatrix} 0 & 0 & 1 & g+d_3 \\ 0 & -1 & 0 & -d_2 \\ 1 & 0 & 0 & d_1 \\ 0 & 0 & 0 & 1 \end{bmatrix}$

Table 4. Forward Displacement Solutions for KS 6 to 13

From the forward displacement solution presented in Table 3 for KS 1, the following relation exists:

$$\begin{Bmatrix} c_1(c_2f+s_{23}g) \\ s_1(c_2f+s_{23}g) \\ s_2f-c_{23}g \\ 1 \end{Bmatrix} = \begin{Bmatrix} p_x \\ p_y \\ p_z \\ 1 \end{Bmatrix} \tag{5}$$

where the left-hand-side of equation (5) is the last column of ${}^{0}_{sph}\mathbf{T}$. Pre-multiplying both sides of equation (5) by ${}^{1}_{0}\mathbf{T} = \left({}^{0}_{1}\mathbf{T}\right)^{-1}$ isolates θ_1 to the right-hand-side of the expression:

$$\begin{Bmatrix} c_2f+s_{23}g \\ 0 \\ s_2f-c_{23}g \\ 1 \end{Bmatrix} = \begin{Bmatrix} c_1p_x+s_1p_y \\ -s_1p_x+c_1p_y \\ p_z \\ 1 \end{Bmatrix} \tag{6}$$

From the second row of equation (6), a solution for θ_1 can be found as:

$$\theta_1 = \text{atan2}(p_y, p_x) \text{ or } \theta_1 = \text{atan2}(-p_y, -p_x) \tag{7}$$

where atan2 denotes a quadrant corrected arctangent function (Paul, 1981). Squaring and adding the first three rows of equation (6) allows an expression for s_3 to be found thus yielding a solution for θ_3 of:

$$\theta_3 = \text{atan2}\left(s_3, \pm\sqrt{1-s_3^2}\right), \text{ where } s_3 = \frac{p_x^2 + p_y^2 + p_z^2 - f^2 - g^2}{2fg} \tag{8}$$

From rows one and three of equation (6), after substituting $c_{23} = c_2c_3 - s_2s_3$ and $s_{23} = s_2c_3 + c_2s_3$, expressions for s_2 and c_2 can be found thus yielding a solution for θ_2 of:

$$\theta_2 = \text{atan2}(s_2, c_2) \tag{9}$$

where

$$s_2 = \frac{c_3g\left(c_1p_x + s_1p_y\right) + \left(f + s_3g\right)p_z}{f^2 + g^2 + 2s_3fg}$$

$$c_2 = \frac{\left(f + s_3g\right)\left(c_1p_x + s_1p_y\right) - c_3gp_z}{f^2 + g^2 + 2s_3fg}$$

A similar procedure can be followed for the other KS layouts. Inverse displacement solutions for all 13 of the KS layouts are summarized in Tables 5 and 6.

KS	Inverse Displacement Solutions
1	$\theta_1 = \text{atan2}(p_y, p_x) \text{ or } \text{atan2}(-p_y, -p_x)$ $\theta_3 = \text{atan2}\left(s_3, \pm\sqrt{1-s_3^2}\right), \text{where } s_3 = \dfrac{p_x^2 + p_y^2 + p_z^2 - f^2 - g^2}{2fg}$ $\theta_2 = \text{atan2}(s_2, c_2),$ $\text{where } s_2 = \dfrac{c_3 g(c_1 p_x + s_1 p_y) + (f + s_3 g) p_z}{f^2 + g^2 + 2 s_3 fg} \;\&\; c_2 = \dfrac{(f + s_3 g)(c_1 p_x + s_1 p_y) - c_3 g p_z}{f^2 + g^2 + 2 s_3 fg}$
2	$\theta_3 = \text{atan2}\left(s_3, \pm\sqrt{1-s_3^2}\right), \text{where } s_3 = \dfrac{p_x^2 + p_y^2 + p_z^2 - f^2 - g^2}{2fg}$ $\theta_2 = \text{atan2}\left(s_2, \pm\sqrt{1-s_2^2}\right), \text{where } s_2 = \dfrac{p_z}{f + s_3 g}$ $\theta_1 = \text{atan2}(s_1, c_1), \text{where } s_1 = \dfrac{(f + s_3 g) c_2 p_y + c_3 g p_x}{p_x^2 + p_y^2} \;\&\; c_1 = \dfrac{(f + s_3 g) c_2 p_x - c_3 g p_y}{p_x^2 + p_y^2}$
3	$\theta_3 = \text{atan2}\left(\pm\sqrt{1-c_3^2}, c_3\right), \text{where } c_3 = \dfrac{p_x^2 + p_y^2 + p_z^2 - f^2 - g^2}{2fg}$ $\theta_2 = \text{atan2}\left(s_2, \pm\sqrt{1-s_2^2}\right), \text{where } s_2 = \dfrac{p_z}{s_3 g}$ $\theta_1 = \text{atan2}(s_1, c_1), \text{where } s_1 = \dfrac{(f + c_3 g) p_x + c_2 s_3 g p_y}{p_x^2 + p_y^2} \;\&\; c_1 = \dfrac{c_2 s_3 g p_x - (f + c_3 g) p_y}{p_x^2 + p_y^2}$
4	$\theta_3 = \text{atan2}\left(\pm\sqrt{1-c_3^2}, c_3\right), \text{where } c_3 = p_z / g$ $\theta_2 = \text{atan2}\left(\pm\sqrt{1-c_2^2}, c_2\right), \text{where } c_2 = \dfrac{f^2 + s_3^2 g^2 - p_x^2 - p_y^2}{2 s_3 fg}$ $\theta_1 = \text{atan2}(s_1, c_1), \text{where } s_1 = \dfrac{s_2 s_3 g p_x + (f - c_2 s_3 g) p_y}{p_x^2 + p_y^2}$ $\& \; c_1 = \dfrac{(f - c_2 s_3 g) p_x - s_2 s_3 g p_y}{p_x^2 + p_y^2}$
5	$\theta_1 = \text{atan2}(p_y, p_x) \pm \text{atan2}\left(\sqrt{p_x^2 + p_y^2 - (f + c_2 s_3 g)^2}, f + c_2 s_3 g\right),$ $\text{where } c_2 s_3 = \dfrac{p_x^2 + p_y^2 + p_z^2 - f^2 - g^2}{2fg}$ $\theta_3 = \text{atan2}\left(\pm\sqrt{1-c_3^2}, c_3\right), \text{where } c_3 = (s_1 p_x - c_1 p_y) / g$ $\theta_2 = \text{atan2}(s_2, c_2), \text{where } s_2 = \dfrac{p_z}{s_3 g} \;\&\; c_2 = \dfrac{c_1 p_x + s_1 p_y - f}{s_3 g}$

Table 5. Inverse Displacement Solutions for KS 1 to 5

KS	Inverse Displacement Solutions
6	$d_1 = p_z \pm \sqrt{-p_x^2 - p_y^2 + g^2}$ $\theta_3 = \text{atan2}\left(\pm\sqrt{1-c_3^2}, c_3\right)$, where $c_3 = (p_z - d_1)/g$ $\theta_2 = \text{atan2}(s_2, c_2)$, where $s_2 = \dfrac{-p_y}{s_3 g}$ & $c_2 = \dfrac{-p_x}{s_3 g}$
7	$d_1 = p_z$ $\theta_3 = \text{atan2}\left(s_3, \pm\sqrt{1-s_3^2}\right)$, where $s_3 = \dfrac{p_x^2 + p_y^2 - f^2 - g^2}{2fg}$ $\theta_2 = \text{atan2}(s_2, c_2)$, where $s_2 = \dfrac{c_3 g p_x + (f + s_3 g) p_y}{(f + s_3 g)^2 + c_3^2 g^2}$ & $c_2 = \dfrac{(f + s_3 g) p_x - c_3 g p_y}{(f + s_3 g)^2 + c_3^2 g^2}$
8	$\theta_1 = \text{atan2}(p_y, p_x)$ or $\text{atan2}(-p_y, -p_x)$ $d_3 = \pm\sqrt{p_x^2 + p_y^2 + p_z^2} - g$ $\theta_2 = \text{atan2}(s_2, c_2)$, where $s_2 = \dfrac{-c_1 p_x - s_1 p_y}{d_3 + g}$ & $c_2 = \dfrac{p_z}{d_3 + g}$
9	$\theta_1 = \text{atan2}(p_x, -p_y)$ or $\text{atan2}(-p_x, p_y)$ $d_2 = s_1 p_x - c_1 p_y \pm \sqrt{g^2 - p_z^2}$ $\theta_3 = \text{atan2}(s_3, c_3)$, where $s_3 = -p_z/g$ & $c_3 = (s_1 p_x - c_1 p_y - d_2)/g$
10	$\theta_3 = \text{atan2}\left(\pm\sqrt{1-c_3^2}, c_3\right)$, where $c_3 = p_z/g$ $d_2 = \pm\sqrt{p_x^2 + p_y^2 - s_3^2 g^2}$ $\theta_1 = \text{atan2}(s_1, c_1)$, where $s_1 = \dfrac{-s_3 g p_y + d_2 p_x}{p_x^2 + p_y^2}$ & $c_1 = \dfrac{-s_3 g p_x - d_2 p_y}{p_x^2 + p_y^2}$
11	$d_1 = p_z$ $d_3 = \pm\sqrt{p_x^2 + p_y^2} - g$ $\theta_2 = \text{atan2}(s_2, c_2)$, where $s_2 = \dfrac{p_x}{d_3 + g}$ & $c_2 = \dfrac{-p_y}{d_3 + g}$
12	$d_2 = -p_y$ $d_1 = p_z \pm \sqrt{-p_x^2 + g^2}$ $\theta_3 = \text{atan2}(s_3, c_3)$, where $s_3 = -p_x/g$ & $c_3 = (p_z - d_1)/g$
13	$d_3 = p_x - g$ $d_2 = -p_y$ $d_1 = p_z$

Table 6. Inverse Displacement Solutions for KS 6 to 13

Referring to Tables 5 and 6, for KS 1 to 6, 8, 9, and 10, up to four possible solutions exist to the inverse displacement problem. For KS 7, 11, and 12, up to two possible solutions exist for the inverse displacement problem. For KS 13 there is only one solution to the inverse displacement problem.

For the inverse displacement solutions presented, undefined configurations occur when the spherical wrist centre of the arm intersects either the first or second joint axes, provided the axes are for a revolute joint. In such a configuration, the inverse solution becomes undefined, i.e., an infinity of possible solutions exist. Looking at KS 3 of Figure 5 as an example, if $s_3 = 0$ as illustrated, the spherical wrist centre intersects the second joint axis and the solution for θ_2 becomes arbitrary. Similarly, if $p_x = p_y = 0$, the spherical wrist centre intersects the first joint axis and the solution for θ_1 becomes arbitrary.

Table 7 reports all of the undefined configurations for the KS family of layouts. If an undefined configuration was encountered, a value would be assigned to the arbitrary joint displacement.

KS	Undefined Configurations	KS	Undefined Configurations
1	$p_x = p_y = 0 \Rightarrow \theta_1$ is arbitrary $f^2 + g^2 + 2s_3 fg = 0 \Rightarrow \theta_2$ is arbitrary	2	$p_x = p_y = 0 \Rightarrow \theta_1$ is arbitrary $f + s_3 g = 0 \Rightarrow \theta_2$ is arbitrary
3	$p_x = p_y = 0 \Rightarrow \theta_1$ is arbitrary $s_3 = 0 \Rightarrow \theta_2$ is arbitrary	4	$p_x = p_y = 0 \Rightarrow \theta_1$ is arbitrary $s_3 = 0 \Rightarrow \theta_2$ is arbitrary
5	$p_x = p_y = 0 \Rightarrow \theta_1$ is arbitrary $s_3 = 0 \Rightarrow \theta_2$ is arbitrary	6	$s_3 = 0 \Rightarrow \theta_2$ is arbitrary
7	$(f + s_3 g)^2 + c_3^2 g^2 = 0 \Rightarrow \theta_2$ is arbitrary	8	$p_x = p_y = 0 \Rightarrow \theta_1$ is arbitrary $d_3 + g = 0 \Rightarrow \theta_2$ is arbitrary
9	$p_x = p_y = 0 \Rightarrow \theta_1$ is arbitrary	10	$p_x = p_y = 0 \Rightarrow \theta_1$ is arbitrary
11	$d_3 + g = 0 \Rightarrow \theta_2$ is arbitrary	12	None
13	None		

Table 7. Undefined Configurations for the Inverse Displacement Solutions of the KS Layouts

5. Discussion

5.1 Application of the KS Layouts

The KS family of layouts can be used as main-arms for serial manipulators or as branches of parallel manipulators. For example, KS 1 is a common main-arm layout for numerous industrial serial manipulators. KS 4 is the branch configuration used in the RSI Research 6-DOF Master Controller parallel joystick (Podhorodeski, 1991). KS 8 is a very common layout used in many parallel manipulators including the Stewart-Gough platform (Stewart, 1965-66). KS 13 is the layout used in Cartesian manipulators.
The choice of which KS layout to use for a manipulator would depend on factors such as the shape of the desired workspace, the ease of manufacture of the manipulator, the task required, etc. For example, layout KS 1 provides a large spherical workspace. Having the second and third joints parallel in KS 1 allows for the motors of the main-arm to be mounted close to the base and a simple drive-train can used to move the third joint.

5.2 Reconfigurable Manipulators

KS layouts are also very useful for reconfigurable manipulators. Podhorodeski and Nokleby (2000) presented a Reconfigurable Main-Arm (RMA) manipulator capable of configuring into all five KS layouts comprised of revolute only joints (KS 1 to 5). Depending on the task required, one of the five possible layouts can be selected.
Yang, et al. (2001) showed how KS branches are useful for modular reconfigurable parallel manipulators.

5.3 Application of the Presented Displacement Solutions

5.3.1 Serial Manipulators

If a KS layout is to be used as a main-arm of a serial manipulator, the spherical wrist needs to be actuated. Figure 8 shows the zero-displacement configuration and Table 8 the D&H parameters for the common roll-pitch-roll spherical-wrist layout. The wrist shown in Figure 8 can be attached to any of the KS layouts.

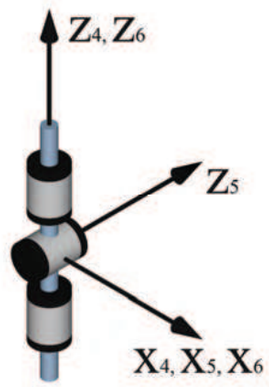

Figure 8. Zero-Displacement Diagram for the Roll-Pitch-Roll Spherical Wrist

F_{j-1}	α_{j-1}	a_{j-1}	d_j	θ_j	F_j
F_{sph}	0	0	0	θ_4	F_4
F_4	$-\pi/2$	0	0	θ_5	F_5
F_5	$\pi/2$	0	0	θ_6	F_6

Table 8. D&H Parameters for the Roll-Pitch-Roll Spherical Wrist

For the KS family of layouts with a spherical wrist, the forward displacement solution is:

$$ {}^{0}_{ee}\mathbf{T} = \left({}^{0}_{1}\mathbf{T}\ {}^{1}_{2}\mathbf{T}\ {}^{2}_{3}\mathbf{T}\ {}^{3}_{sph}\mathbf{T}\right)\left({}^{sph}_{4}\mathbf{T}\ {}^{4}_{5}\mathbf{T}\ {}^{5}_{6}\mathbf{T}\right){}^{6}_{ee}\mathbf{T} = {}^{0}_{sph}\mathbf{T}\,{}^{sph}_{6}\mathbf{T}\,{}^{6}_{ee}\mathbf{T} \tag{10} $$

where ${}^{6}_{ee}\mathbf{T}$ is the homogeneous transformation describing the end-effector frame F_{ee} with respect to frame F_6 and would be dependent on the type of tool attached, ${}^{0}_{sph}\mathbf{T}$ is defined in equation (3), and ${}^{sph}_{6}\mathbf{T}$ is:

$$ {}^{sph}_{6}\mathbf{T} = \begin{bmatrix} c_4c_5c_6 - s_4s_6 & -c_4c_5s_6 - s_4c_6 & c_4s_5 & 0 \\ s_4c_5c_6 + c_4s_6 & -s_4c_5s_6 + c_4c_6 & s_4s_5 & 0 \\ -s_5c_6 & s_5s_6 & c_5 & 0 \\ 0 & 0 & 0 & 1 \end{bmatrix} \tag{11} $$

For a 6-joint serial manipulator, Pieper (1968) demonstrated that for a manipulator with three axes intersecting, a closed-form solution to the inverse displacement problem can be found. As demonstrated by Paul (1981), for a 6-joint manipulator with a spherical wrist, the solutions for the main-arm and wrist displacements can be solved separately. Therefore, the presented inverse

displacement solutions for the KS family of layouts (see Section 4.2) can be used to solve for the main-arm joint displacements for serial manipulators that use KS layouts as their main-arm and have a spherical wrist.

For the inverse displacement solution of the main-arm joints, the location ($^{0}\mathbf{p}_{o_0 \to o_6}$) and orientation ($^{0}_{6}\mathbf{R}$) of frame F_6 with respect to the base frame in terms of the known value $^{0}_{ee}\mathbf{T}$ can be found from:

$$^{0}_{6}\mathbf{T} = {}^{0}_{ee}\mathbf{T}\left({}^{6}_{ee}\mathbf{T}\right)^{-1} = {}^{0}_{ee}\mathbf{T}\,{}^{ee}_{6}\mathbf{T} = \begin{bmatrix} & {}^{0}_{6}\mathbf{R} & & {}^{0}\mathbf{p}_{o_0 \to o_6} \\ 0 & 0 & 0 & 1 \end{bmatrix} \tag{12}$$

where $^{ee}_{6}\mathbf{T}$ is constant and known. Since the manipulator has a spherical wrist:

$${}^{0}\mathbf{p}_{o_0 \to o_{sph}} = {}^{0}\mathbf{p}_{o_0 \to o_6} = {}^{0}\mathbf{p}_{o_0 \to o_5} = {}^{0}\mathbf{p}_{o_0 \to o_4} = \begin{Bmatrix} p_x \\ p_y \\ p_z \end{Bmatrix} \tag{13}$$

where p_x, p_y, and p_z are found from equation (12). The inverse displacement solutions for the KS family of layouts discussed in Section 4.2 can now be used to solve for the main-arm joint displacements.

For the inverse displacement solution of the spherical wrist joints, in terms of the known value $^{0}_{ee}\mathbf{T}$, the orientation of F_6 with respect to the base frame, $^{0}_{6}\mathbf{R}$, was defined in equation (12). Note that:

$${}^{3}_{6}\mathbf{R} = {}^{0}_{3}\mathbf{R}^{T}\,{}^{0}_{6}\mathbf{R} = {}^{3}_{0}\mathbf{R}\,{}^{0}_{6}\mathbf{R} = \begin{bmatrix} r_{11} & r_{12} & r_{13} \\ r_{21} & r_{22} & r_{23} \\ r_{31} & r_{32} & r_{33} \end{bmatrix} \tag{14}$$

Since the main arm joint displacements were solved above, the elements of matrix $^{3}_{0}\mathbf{R}$ are known values and thus the right-hand-side of equation (14) is known, i.e., r_{ij}, i = 1 to 3 and j = 1 to 3, are known values.

Substituting the elements of the rotation matrix $^{3}_{6}\mathbf{R} = {}^{3}_{sph}\mathbf{R}\,{}^{sph}_{6}\mathbf{R}$ into equation (14) yields:

$${}^{3}_{6}\mathbf{R} = {}^{3}_{sph}\mathbf{R}\,{}^{sph}_{6}\mathbf{R} = {}^{3}_{sph}\mathbf{R}\begin{bmatrix} c_4c_5c_6 - s_4s_6 & -c_4c_5s_6 - s_4c_6 & c_4s_5 \\ s_4c_5c_6 + c_4s_6 & -s_4c_5s_6 + c_4c_6 & s_4s_5 \\ -s_5c_6 & s_5s_6 & c_5 \end{bmatrix} = \begin{bmatrix} r_{11} & r_{12} & r_{13} \\ r_{21} & r_{22} & r_{23} \\ r_{31} & r_{32} & r_{33} \end{bmatrix} \tag{15}$$

where ${}^{3}_{sph}\mathbf{R}$ is dependent on the D&H parameter α_3 for the manipulator, i.e.:

$$
\begin{aligned}
{}^{3}_{sph}\mathbf{R} &= \begin{bmatrix} 1 & 0 & 0 \\ 0 & 1 & 0 \\ 0 & 0 & 1 \end{bmatrix}, \text{if } \alpha_3 = 0 \\
{}^{3}_{sph}\mathbf{R} &= \begin{bmatrix} 1 & 0 & 0 \\ 0 & 0 & -1 \\ 0 & 1 & 0 \end{bmatrix}, \text{if } \alpha_3 = \frac{\pi}{2} \\
{}^{3}_{sph}\mathbf{R} &= \begin{bmatrix} 1 & 0 & 0 \\ 0 & 0 & 1 \\ 0 & -1 & 0 \end{bmatrix}, \text{if } \alpha_3 = -\frac{\pi}{2}
\end{aligned}
\tag{16}
$$

Equation (15) can be used to derive expressions for the wrist joint displacements θ_4, θ_5, and θ_6. For example, if $\alpha_3 = \pi/2$, equation (15) becomes:

$$
\begin{bmatrix} c_4c_5c_6 - s_4s_6 & -c_4c_5s_6 - s_4c_6 & c_4s_5 \\ s_5c_6 & -s_5s_6 & -c_5 \\ s_4c_5c_6 + c_4s_6 & -s_4c_5s_6 + c_4c_6 & s_4s_5 \end{bmatrix} = \begin{bmatrix} r_{11} & r_{12} & r_{13} \\ r_{21} & r_{22} & r_{23} \\ r_{31} & r_{32} & r_{33} \end{bmatrix} \tag{17}
$$

Using element (2, 3) of equation (17) allows θ_5 to be solved as:

$$
\theta_5 = \text{atan2}\left(\pm\sqrt{1-c_5^2}, c_5\right), \text{where } c_5 = -r_{23} \tag{18}
$$

Using elements (1, 3) and (3, 3) of equation (17) allows θ_4 to be solved as:

$$
\theta_4 = \text{atan2}(s_4, c_4), \text{where } s_4 = \frac{r_{33}}{s_5} \;\&\; c_4 = \frac{r_{13}}{s_5} \tag{19}
$$

Using elements (3, 1) and (3, 2) of equation (17) allows θ_6 to be solved as:

$$
\theta_6 = \text{atan2}(s_6, c_6) \tag{20}
$$

where

$$
s_6 = \frac{-c_4r_{31} + s_4c_5r_{32}}{-s_4^2c_5^2 - c_4^2}
$$

$$
c_6 = \frac{-s_4c_5r_{31} - c_4r_{32}}{-s_4^2c_5^2 - c_4^2}
$$

Note that if $s_5 = 0$, joint axes 4 and 6 are collinear and the solutions for θ_4 and θ_6 are not unique. In this case, θ_4 can be chosen arbitrarily and θ_6 can be solved for.
Similar solutions can be found for the cases where α_3 equals 0 and $-\pi/2$.

5.3.2 Parallel Manipulators

Two frames common to the branches of the parallel manipulator are established, one frame attached to the base (F_{base}) and the other attached to the platform (F_{plat}). The homogeneous transformations from the base frame F_{base} to the base frame of each of the m branches F_{0_i} are denoted ${}^{base}_{0_i}\mathbf{T}$, i = 1 to m. The homogeneous transformations from the platform frame F_{plat} to the m passive spherical group frames F_{sph_i} are denoted ${}^{plat}_{sph_i}\mathbf{T}$, i = 1 to m. Note that for a given parallel manipulator all ${}^{base}_{0_i}\mathbf{T}$ and ${}^{plat}_{sph_i}\mathbf{T}$ would be known and would be constant.
For the inverse displacement solution, for the i^{th} branch, the location and orientation of the spherical wrist frame, F_{sph_i}, with respect to the base frame of the branch, F_{0_i}, in terms of the known value ${}^{base}_{plat}\mathbf{T}$ can be found from:

$$ {}^{0_i}_{sph_i}\mathbf{T} = \left({}^{base}_{0_i}\mathbf{T}\right)^{-1} {}^{base}_{plat}\mathbf{T}\, {}^{plat}_{sph_i}\mathbf{T} = {}^{0_i}_{base}\mathbf{T}\, {}^{base}_{plat}\mathbf{T}\, {}^{plat}_{sph_i}\mathbf{T} = \begin{bmatrix} {}^{0_i}_{sph_i}\mathbf{R} & {}^{0_i}\mathbf{p}_{o_{0_i}\to o_{sph_i}} \\ 0 \quad 0 \quad 0 & 1 \end{bmatrix} \tag{21} $$

where ${}^{0_i}_{sph_i}\mathbf{R}$ is the orientation of F_{sph_i} with respect to F_{0_i} and ${}^{0_i}\mathbf{p}_{o_{0_i}\to o_{sph_i}}$ is the position vector from the origin of F_{0_i} to the origin of F_{sph_i} with respect to F_{0_i}. The position vector is defined as:

$$ {}^{0_i}\mathbf{p}_{o_{0_i}\to o_{sph_i}} = \begin{Bmatrix} p_{x_i} \\ p_{y_i} \\ p_{z_i} \end{Bmatrix} \tag{22} $$

where p_{x_i}, p_{y_i}, and p_{z_i} are known values. The inverse displacement solutions for the KS family of layouts shown in Section 4.2 can then be used to solve for the joint displacements for branches i =1 to m.

Unlike the forward displacement problem of serial manipulators, the forward displacement problem of parallel manipulators is challenging. Raghavan

(1993) showed that for the general 6-61 Stewart-Gough platform up to 40 solutions could exist to the forward displacement problem. Note that the notation *i-j* denotes the number of connection points of the branches at the base and platform, respectively.
Innocenti and Parenti-Castelli (1990) showed that for a class of parallel manipulators that have the branches connected at three distinct points on the end-effector platform (e.g., 6-3 and 3-3 layouts), the forward displacement problem can be reduced to a 16th order polynomial of one variable leading to a maximum of 16 possible solutions to the forward displacement problem.
Numerous researchers (e.g., Inoue, et al. (1986); Waldron, et al. (1989); Cheok, et al. (1993); Merlet (1993); Notash and Podhorodeski (1994 and 1995); and Baron and Angeles (2000)) have shown that utilizing redundant sensing in parallel manipulators is necessary to achieve a unique solution to the forward displacement problem. For the purposes of the solutions presented here, it is assumed that the manipulator is redundantly sensed and that the positions of the passive spherical groups ($\mathbf{p}_i$, i = 1 to m) would be known.

Noting that:

$$ {}^{base}_{plat}\mathbf{T} = \begin{bmatrix} {}^{base}_{plat}\mathbf{R} & {}^{base}\mathbf{p}_{o_{base}\rightarrow o_{plat}} \\ 0 \quad 0 \quad 0 & 1 \end{bmatrix} \tag{23} $$

For 6-3 and 3-3 layouts, the origin of F_{plat} can be found as:

$$ {}^{base}\mathbf{p}_{o_{base}\rightarrow o_{plat}} = \frac{{}^{base}(\mathbf{p}_1 + \mathbf{p}_2 + \mathbf{p}_3)}{3} \tag{24} $$

where $\mathbf{p}_1$, $\mathbf{p}_2$, and $\mathbf{p}_3$ are the positions of the passive spherical groups. The positions of the passive spherical groups can be found using the solutions presented in Tables 3 to 4.
The orientation of the platform frame can be found as:

$$ {}^{base}_{plat}\mathbf{R} = {}^{base}[\mathbf{n} \quad \mathbf{o} \quad \mathbf{a}] \tag{25} $$

where

[1] Note that the notation *i-j* denotes the number of connection points of the branches at the base and platform, respectively.

$$^{base}\mathbf{n}=\ ^{base}\left(\frac{\mathbf{p}_3-\mathbf{p}_2}{\|\mathbf{p}_3-\mathbf{p}_2\|}\right)$$

$$^{base}\mathbf{a}=\frac{^{base}\mathbf{n}\times\ ^{base}\mathbf{c}}{\left\|^{base}\mathbf{n}\times\ ^{base}\mathbf{c}\right\|}$$

$$^{base}\mathbf{o}=^{base}\mathbf{a}\times\ ^{base}\mathbf{n}$$

with

$$^{base}\mathbf{c}=\ ^{base}\left(\frac{\mathbf{p}_1-\mathbf{p}_2}{\|\mathbf{p}_1-\mathbf{p}_2\|}\right)$$

For 6-6 and 3-6 layouts, the origin of F_{plat} can be found as:

$$^{base}\mathbf{p}_{o_{base}\to o_{plat}}=\frac{^{base}\left(\mathbf{p}_1+\mathbf{p}_2+\mathbf{p}_3+\mathbf{p}_4+\mathbf{p}_5+\mathbf{p}_6\right)}{6} \tag{26}$$

where $\mathbf{p}_1$ to $\mathbf{p}_6$ are the positions of the passive spherical groups. Note that it is assumed that the passive spherical groups are symmetrically distributed about the platform. The positions of the passive spherical groups can be found using the solutions presented in Tables 3 and 4.
The orientation of the platform frame can be found as:

$$^{base}_{plat}\mathbf{R}=^{base}\left[\mathbf{n}\quad\mathbf{o}\quad\mathbf{a}\right] \tag{27}$$

where

$$^{base}\mathbf{n}=\ ^{base}\left(\frac{\mathbf{p}_c-\mathbf{p}_b}{\|\mathbf{p}_c-\mathbf{p}_b\|}\right)$$

$$^{base}\mathbf{a}=\frac{^{base}\mathbf{n}\times\ ^{base}\mathbf{c}}{\left\|^{base}\mathbf{n}\times\ ^{base}\mathbf{c}\right\|}$$

$$^{base}\mathbf{o}=^{base}\mathbf{a}\times\ ^{base}\mathbf{n}$$

with

$$^{base}\mathbf{c}=\frac{\mathbf{p}_a-\mathbf{p}_b}{\|\mathbf{p}_a-\mathbf{p}_b\|}$$

$$\mathbf{p}_a=\left(\mathbf{p}_1+\mathbf{p}_2\right)/2$$

$$\mathbf{p}_b=\left(\mathbf{p}_3+\mathbf{p}_4\right)/2$$

$$\mathbf{p}_c=\left(\mathbf{p}_5+\mathbf{p}_6\right)/2$$

6. Conclusions

The complete set of layouts belonging to a kinematically simple (KS) family of spatial joint layouts were presented. The considered KS layouts were defined as ones in which the manipulator (or branch of a parallel manipulator) incorporates a spherical group of joints at the wrist with a main-arm comprised of successfully parallel or perpendicular joints with no unnecessary offsets or lengths between joints. It was shown that there are
13 layouts having unique kinematics belonging to the KS family: five layouts comprised of three revolute joints; five layouts comprised of two revolute joints and one prismatic joint; two layouts comprised of one revolute joint and two prismatic joints; and one layout comprised of three prismatic joints. In addition, it was shown that there are a further five kinematically-simple layouts having unique joint structures, but kinematics identical to one of the 13 KS layouts.
Zero-displacement diagrams, D&H parameters, and the complete forward and inverse displacement solutions for the KS family of layouts were presented. It was shown that for the inverse displacement problem up to four possible solutions exist for KS 1 to 6, 8, 9, and 10, up to two possible solutions exist for KS 7, 11, and 12, and only one solution exists for KS 13. The application of the KS family of joint layouts and the application of the presented forward and inverse displacement solutions to both serial and parallel manipulators was discussed.

Acknowledgements

The authors wish to thank the Natural Sciences and Engineering Research Council (NSERC) of Canada for providing funding for this research.

7. References

Baron, L. & Angeles, J. (2000). The Direct Kinematics of Parallel Manipulators Under Joint-Sensor Redundancy. *IEEE Transactions on Robotics and Automation*, Vol. 16, No. 1, pp. 12-19.

Cheok, K. C.; Overholt, J. L. & Beck, R. R. (1993). Exact Methods for Determining the Kinematics of a Stewart Platform Using Additional Displacement Sensors. *Journal of Robotic Systems*, Vol. 10, No. 5, pp. 689-707.

Craig, J. J. (1989). *Introduction To Robotics: Mechanics and Control - Second Edition*, Addison-Wesley Publishing Company, Don Mills, Ontario, Canada.

Denavit, J. & Hartenberg, R. S. (1955). A Kinematic Notation for Lower-Pair Mechanisms Based on Matrices. *Transactions of the ASME, Journal of Applied Mechanics*, June, pp. 215-221.

Innocenti, C. & Parenti-Castelli, V. (1990). Direct Position Analysis of the Stewart Platform Mechanism. *Mechanism and Machine Theory*, Vol. 25, No. 6, pp. 611-621.

Inoue, H.; Tsusaka, Y. & and Fukuizumi, T. (1986). Parallel Manipulator, In: Robotics Research: The Third International Symposium, Faugeras, O. D. & Giralt, G., (Ed.), pp. 321-327, MIT Press, Cambridge, Massachusetts, USA.

Merlet, J.-P. (1993). Closed-Form Resolution of the Direct Kinematics of Parallel Manipulators Using Extra Sensors Data, *Proceedings of the 1993 IEEE International Conference on Robotics and Automation - Volume 1*, May 2-6, 1993, Atlanta, Georgia, USA, pp. 200-204.

Notash, L. & Podhorodeski, R. P. (1994). Complete Forward Displacement Solutions for a Class of Three-Branch Parallel Manipulators. *Journal of Robotic Systems*, Vol. 11, No. 6, pp. 471-485.

Notash, L. & Podhorodeski, R. P. (1995). On the Forward Displacement Problem of Three-Branch Parallel Manipulators. *Mechanism and Machine Theory*, Vol. 30, No. 3, pp. 391-404.

Paul, R. P. (1981). *Robot Manipulators: Mathematics, Programming, and Control*, MIT Press, Cambridge, Massachusetts, USA.

Pieper, D. L. (1968). *The Kinematics of Manipulators Under Computer Control*. Ph.D. Dissertation, Stanford University, Stanford, California, USA.

Podhorodeski, R. P. (1991). A Screw Theory Based Forward Displacement Solution for Hybrid Manipulators, *Proceedings of the 2nd National Applied Mechanisms and Robotics Conference - Volume I*, November 3-6, 1991, Cincinnati, Ohio, USA, pp. IIIC.2--1 - IIIC.2-7.

Podhorodeski, R. P. (1992). Three Branch Hybrid-Chain Manipulators: Structure, Displacement, Uncertainty and Redundancy Related Concerns, *Proceedings of the 3rd Workshop on Advances in Robot Kinematics*, September 7-9, 1992, Ferrara, Italy, pp. 150-156.

Podhorodeski, R. P. & Nokleby, S. B. (2000). Reconfigurable Main-Arm for Assembly of All Revolute-Only Kinematically Simple Branches. *Journal of Robotic Systems*, Vol. 17, No. 7, pp. 365-373.

Podhorodeski, R. P. & Pittens, K. H. (1992). A Class of Hybrid-Chain Manipulators Based on Kinematically Simple Branches, *Proceedings of the 1992 ASME Design Technical Conferences - 22nd Biennial Mechanisms Conference*, September 13-16, 1992, Phoenix, Arizona, USA, pp. 59-64.

Podhorodeski, R. P. & Pittens, K. H. (1994). A Class of Parallel Manipulators Based on Kinematically Simple Branches. *Transactions of the ASME, Journal of Mechanical Design*, Vol. 116, No. 3, pp. 908-914.

Raghavan, M. (1993). The Stewart Platform of General Geometry Has 40 Configurations. *Transactions of the ASME, Journal of Mechanical Design*, Vol. 115, No. 2, pp. 277-282.

Stewart, D. (1965-66). *A Platform With Six Degrees of Freedom*. Proceedings of the Institution of Mechanical Engineers, Vol. 180, Part 1, No. 15, pp. 371-386.

Waldron, K. J.; Raghavan, M. & Roth, B. (1989). Kinematics of a Hybrid Series-Parallel Manipulation System. *Transactions of the ASME, Journal of Dynamic Systems, Measurement, and Control*, Vol. 111, No. 2, pp. 211-221.

Yang, G.; Chen, I.-M.; Lim, W. K. & Yeo, S. H. (2001). Kinematic Design of Modular Reconfigurable In-Parallel Robots. *Autonomous Robots*, Vol. 10, Issue 1, pp. 83-89.

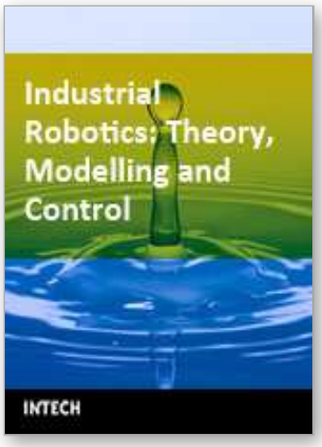

Industrial Robotics: Theory, Modelling and Control

Edited by Sam Cubero

ISBN 3-86611-285-8

Hard cover, 964 pages

Publisher Pro Literatur Verlag, Germany / ARS, Austria

Published online 01, December, 2006

Published in print edition December, 2006

This book covers a wide range of topics relating to advanced industrial robotics, sensors and automation technologies. Although being highly technical and complex in nature, the papers presented in this book represent some of the latest cutting edge technologies and advancements in industrial robotics technology. This book covers topics such as networking, properties of manipulators, forward and inverse robot arm kinematics, motion path-planning, machine vision and many other practical topics too numerous to list here. The authors and editor of this book wish to inspire people, especially young ones, to get involved with robotic and mechatronic engineering technology and to develop new and exciting practical applications, perhaps using the ideas and concepts presented herein.

InTech Europe

University Campus STeP Ri
Slavka Krautzeka 83/A
51000 Rijeka, Croatia
Phone: +385 (51) 770 447
Fax: +385 (51) 686 166
www.intechopen.com

InTech China

Unit 405, Office Block, Hotel Equatorial Shanghai
No.65, Yan An Road (West), Shanghai, 200040, China
中国上海市延安西路65号上海国际贵都大饭店办公楼405单元
Phone: +86-21-62489820
Fax: +86-21-62489821

IntechOpen